The formation and characterisation of redox active and luminescent materials from the electrooxidation of indolizine

PCCP

Cite this: *Phys. Chem. Chem. Phys.*, 2011, **13**, 5235–5241

www.rsc.org/pccp

PAPER

The formation and characterisation of redox active and luminescent materials from the electrooxidation of indolizine†

John B. Henry, Ranald J. MacDonald, Helen S. Gibbad, Hamish McNab and Andrew R. Mount*

Received 23rd November 2010, Accepted 4th February 2011
DOI: 10.1039/c0cp02645j

Indolizine has been synthesised on the small scale with enhanced yield using a novel Flash Vacuum Pyrolysis method. Electrooxidation of indolizine results in the formation of a redox-active film on the electrode surface. Excellent agreement is found between calculated and experimental indolizine oxidation potentials; a combination of fluorescence and electrochemical studies are consistent with the computational prediction that electroxidation results in the formation of three specific and redox active indolizine dimers. The insoluble redox active film is considered to be polymeric and to arise from the further oxidation of these dimers at the electrode. This combination of methods can be used for the characterisation of products formed from the electrooxidation of novel luminescent heteroaromatics synthesised on a small scale and particularly those of interest as redox active species for electrochemical processes and devices.

1. Introduction

N-heteroaromatics such as indoles,[1] pyrroles,[2] carbazoles[3] and indolocarbazoles[4] have received a great deal of attention in recent years as monomers from which redox-active oligomeric and polymeric materials can be produced. Typically these are relatively low cost extended π-conjugated thin-film materials that show semiconducting to conducting electronic properties, redox activity, good processability, attractive mechanical properties and the ready tuning of properties through chemical functionalisation. This makes them of interest for a variety of applications, including the active film in organic electronic devices, sensors, supercapacitors and in electroluminescent materials.[5]

We have recently shown that computational methods can be used to calculate accurately the redox potentials of a range of heteroaromatic molecules.[1d] We have also demonstrated that through consideration of the radical density distribution in oxidised monomer units, plausible mechanisms of electro-oxidative coupling can be deduced which explain the nature of the indole[1d] and indolo[3,2,1-*jk*]carbazole[4d] products, and that it is also possible to distinguish molecules that are not promising candidates for redox active film formation *via* this approach.[6] However, this approach typically requires the electrochemical and/or chemical synthesis of each reactant and product at a sufficient scale for full and unambiguous characterisation of the reaction products, which precludes characterisation of those species with limited solubility and/or those only able to be synthesised on a small scale.

Indolizine (Fig. 1a) is a highly luminescent[7] constitutional isomer of indole, whose electrochemical properties have not been studied previously to our knowledge. The work in this paper shows that a combination of novel small scale synthesis, electrochemical, spectroscopic and computational studies can be used to study the electrooxidation and film formation properties of indolizine, establishing the electrooxidation properties, characterising the resulting products and producing a plausible mechanism to explain the products of electrooxidation.

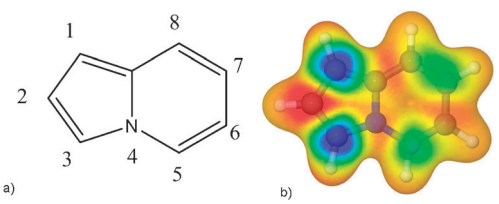

Fig. 1 (a) The structure of indolizine, with the atomic positional numbering convention. (b) The calculated electron spin density distribution mapped onto a 99% electron density isosurface for the radical cation of indolizine. (The colouring scheme is roygb: blue indicates a positive spin density (0.005) while red is negative (−0.001).

School of Chemistry, University of Edinburgh, The King's Buildings, West Mains Road, Edinburgh, EH9 3JJ. E-mail: a.mount@ed.ac.uk; Tel: +44 131 650 4747

† This article is part of the special collection on Interfacial processes and mechanisms in celebration of John Albery's 75th birthday. We also dedicate this work to our colleague and friend Professor Hamish McNab, expert in FVP synthesis, following his untimely death on 15th November 2010.

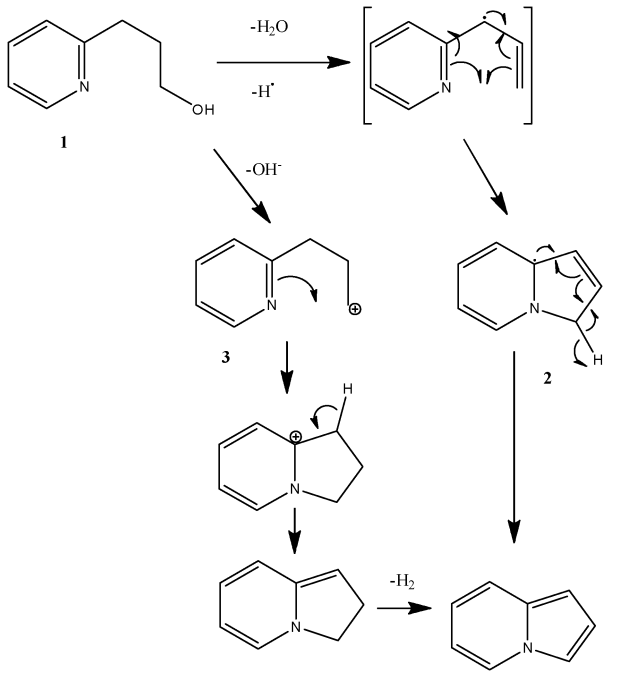

Scheme 1 The proposed FVP coupling mechanisms to form indolizine.

2. Experimental

Electrochemistry

All chemicals were of AnalaR grade or equivalent and were supplied by Sigma Aldrich unless otherwise stated. Electrochemical measurements were performed in background electrolyte solutions of 0.1 M anhydrous $LiClO_4$ in acetonitrile (JT Baker; dried distilled). The reference electrode was made in-house and consisted of a silver wire dipped into a solution of $AgClO_4$ (0.01 M) in background electrolyte solution, with a measured potential of −0.074 V *vs.* the ferrocene/ferrocinium (Fc/Fc^+) couple. All potentials are quoted with respect to this reference unless otherwise stated. The counter electrode was a 2 cm^2 Pt gauze and the working electrode was either a 0.387 cm^2 Pt rotating disc electrode (RDE) or a Pt-Pt rotating ring-disc electrode (RRDE[8]; Oxford Electrodes, disc area 0.387 cm^2, calculated and measured (using the Fc/Fc^+ couple) ring collection efficiency, N_0 = 0.21). These were controlled by an AUTOLAV PGSTAT30 potentiostat (Eco Chemie BV) equipped with GPES 4.9 software and a RRDE motor controller (Oxford Electrodes).

Computation

All calculations were carried out using the software package Gaussian 03[9] running on a SUSe 9.x Linux HPC cluster consisting of 68 AMD Opteron processing cores contained within the EaStChem Research Computing Facility Hare cluster. Default convergence criteria were used for all calculations (maximum force = 0.00045, RMS force = 0.0003, maximum displacement = 0.0018 and RMS displacement = 0.0012). The computational method employed was B3LYP, the Becke[10] Three Parameter Hybrid Functional which utilises the correlation functional of Lee, Yang and Parr[11] and includes both local and non-local terms. For calculations of the electron spin density the unrestricted method uB3LYP was employed. The basis set used in all calculations was 6–311+G(d,p) with acetonitrile solvation modeled with the polarizable continuum model (PCM).[12]

For all molecules a frequency calculation was performed with optimised geometries to ensure that a minimum in the potential energy hypersurface had been reached and to obtain free energies for the molecules at 298 K. The spin density distribution was evaluated by generating cube files for electron density and electron spin. The spin density distribution plots were then made by mapping onto the 99% electron density surface. Output was viewed using Jmol, an open-source Java viewer for chemical structures in 3D (http://www.jmol.org/) and rendered using the Persistence of Vision Raytracer freeware (http://www.povray.org).

Synthesis

Indolizine has been previously synthesised in one step by Boekelheide and Fahrenholtz[13] by thermolysis of 2-pyridine-propanol **1** at 280 °C in the presence of a palladium catalyst; however the yield was low, at 50%. This work has established that FVP of this reagent over a WO_3 catalyst also results in indolizine formation. WO_3 has a mixture of surface Lewis acid and Brønsted acid sites under these conditions[14] which makes it able to facilitate the dehydrogenation, dehydration and cyclisation steps required to form indolizine. The mechanism for indolizine formation on WO_3 (Scheme 1) is postulated as involving either the dehydration of **1**, then cyclisation of the radical formed by H atom abstraction to form **2** or the removal of the hydroxide group through protonation *via* the strong Brønsted acid sites with dehydration to give the cationic intermediate **3**, followed by an intramolecular Friedel Crafts reaction, H atom abstraction and dehydrogenation to give the indolizine product.

The FVP system has been described in detail elsewhere;[4d] a high capacity oil pump (Edwards ED100) was used to maintain system pressure at 0.030 Torr. The inlet tube was heated within a glass Büchi oven to volatilise the reagent, which was passed through a silica tube (30 × 2.5 cm) heated by a tube furnace (Carbolite MTF 12/38/250). The estimated contact time within the hot zone of the furnace of ten milliseconds ensured intramolecular reactions were favoured. A plug of silica wool was inserted into the hot zone to contain the WO_3 catalyst (10 g). The products were condensed in a U-tube cooled with liquid nitrogen. Optimised FVP of **1** (150 mg) was found when using a furnace temperature of 400 °C, an inlet temperature of 100 °C and a pyrolysis time of 30 min. Upon completion of the reaction, the trap was allowed to warm slowly to room temperature. Precipitation of the crude product from aqueous ethanol gave indolizine as a pure white solid (98 mg, 76%); melting point 69–71 °C (lit.[15] 74 °C); δ_H (360 MHz $CDCl_3$) 7.82 (1H, dd, *J* 7.0, *J* 0.9), 7.43–7.21 (2H, m), 6.70 (1H, dd, *J* 3.7, *J* 2.8), 6.55 (1H, ddd, *J* 9.0, *J* 6.5, *J* 0.8) and 6.40–6.26 (2H, m). However, this synthesis was found to be scale limited to 150 mg, most likely due to the loss of the active sites involved in dehydration. Catalyst reactivation could be achieved by roasting in air at 600 °C for one hour.

3. Results and discussion

Calculation of indolizine properties

Using our previously developed computational method of calculating the standard reduction potential and then determining the peak oxidation potential assuming reversible electron transfer,[1d] indolizine has a calculated peak oxidation potential of + 0.38 ± 0.04 V with respect to the ferrocene/ferrocinium (Fc/Fc^+) redox couple. This is much lower than the calculated peak oxidation potential of indole of + 0.82 V *vs.* Fc/Fc^+.[1d] This lower peak oxidation potential suggests that the indolizine radical cation is less reactive than that of indole. For other similar N-heteraromatics it has been established that the assumption of radical–radical coupling on oxidation leads to the correct prediction of the nature of the oligomeric coupling products.[1d,2a,4d] Following this approach, indolizine coupling would be expected to occur at sites of highest electron spin density where there will be the highest propensity for radical–radical coupling, bond formation and rearomatisation to give the neutral dimer through the loss of two protons. It is clear from the calculated electron spin density map of indolizine (Fig. 1b) that the greatest electron spin density is located equally in the 1- and 3-positions of the monomer unit. By analogy with indolocarbazole[4d] this suggests that radical coupling would occur preferentially at these sites, giving three positional isomer dimers as products; the 1,1′-, 1,3′- and 3,3′- products shown in Fig. 2a, b and c, respectively.

As with indole[1d] it is then possible to extend this computational modeling to consider the predicted oxidation potential and likely coupling positions of these dimers. Calculations of the properties of these oligomers are computationally expensive and time consuming, due to the size of each system. The most stable conformation of oxidised and reduced dimers were found to be significantly different and hence the peak oxidation potentials of the dimers were calculated by two different methods. The first was to calculate the difference in energy between the lowest energy conformations of the oxidised and reduced dimers, which assumes that conformational change is an intrinsic part of the electron transfer process and contributes to the thermodynamics of electron transfer. The second was to calculate the oxidation potential assuming that electron transfer occurs without significant conformational change, followed by conformational relaxation to give the most stable state (*i.e.* an EC process). In this case the geometry of dimer radical cation and neutral dimer were constrained to be the same when calculating the oxidation potential. Using the first method the peak oxidation potentials were calculated as −0.31 ± 0.04 V, −0.23 ± 0.04 V and −0.16 ± 0.04 V *vs.* Fc/Fc^+ for the 1,1′-, 1,3′- and 3,3′- dimers respectively, whereas the second method gave peak oxidation potentials of −0.08, 0.02 and 0.15 V ± 0.04 V *vs.* Fc/Fc^+ respectively. Such distinct redox potentials should enable the detection of these species in solution. The calculated barrier heights to conformational change were markedly greater than kT, which favours the EC mechanism and supports calculation by the second method. As all of these oxidation potentials are significantly lower than the calculated peak oxidation potential of the monomer, each would therefore be expected to oxidize at the electrode surface at the potentials required for monomer oxidation. Once again the electron spin density maps provide an indication of the most probable coupling positions of the radical cations formed by one electron oxidation of these dimers. In each case, the greatest electron spin density can be observed (Fig. 2d–f) in both the coupled and uncoupled 1- and 3-positions. This is unlike indole,[1d] whose 3,3′- dimer has the greatest spin density at the positions favouring the asymmetric cyclic trimer electrooxidation product found experimentally. In fact, there is significant delocalisation of the electron spin across the dimer and the amount of electron spin in each position is significantly less than for the indolizine monomer radical cation, which itself is more stable than the indole monomer radical cation. Although it should be remembered that these calculations do not not establish unambiguously whether the oxidised forms of these dimers are stable, giving redox behaviour, as found with indolocarbazole,[4d] or whether oxidation leads to further coupling of these radical cations, these characteristics are likely to favour redox stability.

Indolizine electrochemistry

To test these predictions, the electrooxidation of indolizine in acetonitrile/$LiClO_4$ was studied using cyclic voltametry (CV, Fig. 3). Indolizine was found to have limited solubility in acetonitrile backgound electrolyte of the order of 10 mM; given that heteroaromatic film formation occurs by radical cation coupling, such low concentrations should favour dimer and oligomer formation.[8] The monomer peak oxidation potential was measured to be +0.37 V *vs.* Fc/Fc^+, which is in excellent agreement with the computed value of +0.38 ± 0.04 V *vs.* Fc/Fc^+. Furthermore, while the experimental oxidation peak appears electrochemically reversible (the difference between peak potential and half-peak potential is 54 mV at 298 K, as expected for a reversible one electron oxidation,[16] in support of the method used for calculating the peak oxidation potential[1d]) there is no observed associated reduction peak, suggesting that chemical coupling of the monomer radical cation occurs on oxidation. The first scan also shows a classic nucleation loop near 0.25 V on the return scan, which is indicative of coupling of indolizine and surface film formation. Further CV cycling shows the progressive growth of broad reduction and oxidation peaks centred below 0 V; these peaks were also observed when transferring the electrode to background electrolyte solution and are therefore attributed to oxidation and reduction of a redox active film, which grows progressively thicker with each cycle as the thickness of the film on the electrode increases. These redox peak currents were proportional to CV sweep rate, consistent with a surface film capable of fast redox cycling. Integration of the charge under each CV cycle shows the increase in redox charge to be 7% of the oxidation charge in the previous cycle. The monomer oxidation peak is also seen to be superimposed on a growing oxidation current, indicative of film oxidation. The formed film, visible on the surface, was washed with DMF, DMSO and acetone and found to be insoluble in each of them. This hinders further characterisation but suggests that the film is

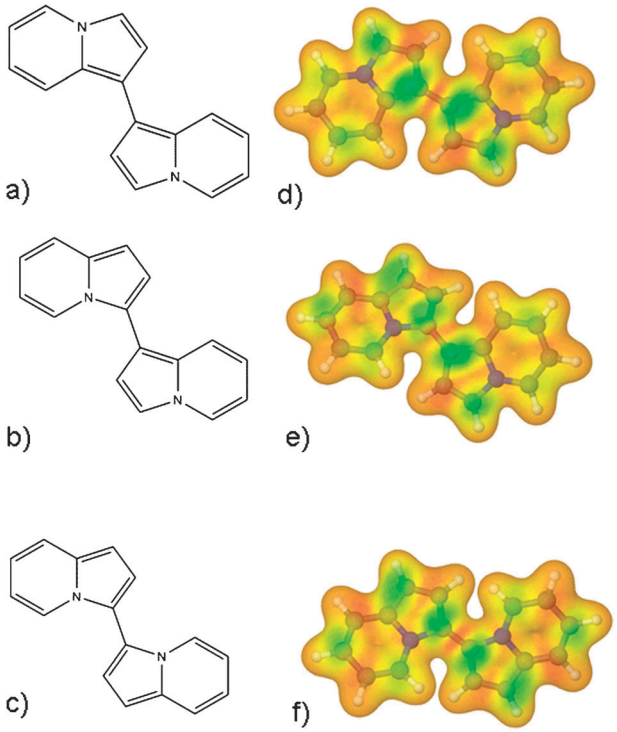

Fig. 2 Structures of the proposed dimer coupling products: (a) 1,1′-diindolizine, (b) 1,3′-diindolizine and (c) 3,3′-diindolizine. For each, typical electron spin density distributions for the radical cations are shown as (d) to (f) respectively, mapped onto the 99% electron density isosurface. (The colouring scheme is the same as Fig. 1).

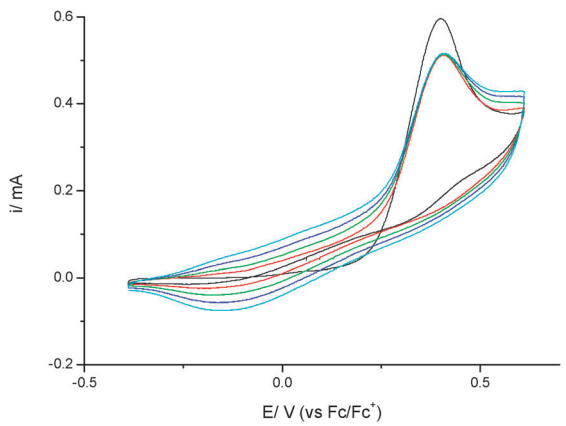

Fig. 3 Typical cyclic voltammograms (CVs) at the stationary RDE for the electroxidation of a solution of 5 mM indolizine in background electrolyte at a sweep rate, v, of 100 mV s^{-1}. The initial direction of sweep is to positive potential, E, from the negative potential limit. Following monomer electrooxidation near 0.4 V in the initial scan (black), this and successive scans show increasing redox peaks at and below 0 V characteristic of redox film formation of increasing thickness.

polymeric in nature. After prolonged electrooxidation above 0.4 V a darkening of the solution was noticed, suggesting the presence of soluble oligomer product in solution. Differential pulse voltammetry (DPV, Fig. 4) showed the presence of two peaks, giving $E_{1/2}$ values of −0.06 and 0.01 V, or peak oxidation values of −0.04 V and 0.04 V respectively, assuming reversible electrochemistry.[16] These values coincide within the estimated calculated error with the 1,1′- and 1,3′- dimer peak oxidation potentials calculated using the second method, suggesting these could be the two soluble redox active products. There is also the suspicion of a third peak above 0.1 V which could be attributable to the third dimer product, but a peak position is not clearly identifiable due to the onset of further oxidation.

Rotating ring-disc electrode (RRDE) methods were then used to characterise further these soluble oligomeric products of the electrooxidation. In these experiments, the ring electrode was held at specific potentials to detect each product whilst voltammetry was carried out at the disc electrode at a rotation speed of 4 Hz (Fig. 5). At ring potentials near $E_R = -0.06$ V it is comforting that the oxidation of the previously formed dimer seen in the DPV studies can be observed and that at disc potentials near and above this potential the ring current drops due to shielding from product oxidation at the the disc electrode.[17] This confirms the stability of these redox active products in solution. After the onset of disc monomer oxidation near 0.3 V increasingly oxidative ring currents can be observed on the ring due to the oxidation of soluble coupling products (Fig. 6). There is little evidence for the reduction of oxidised product at any ring potential. This suggests the soluble products being detected are reduced dimers, formed by the coupling of radical cations in transit between disc and ring. At very low disc currents there is little or no product detected, consistent with a very low concentration of radical cation at the disc precluding coupling and soluble dimer formation. At greater currents the initial increase in ring current is essentially proportional to the disc current, suggesting efficient, quantitative soluble dimer product formation at these low indolizine concentrations. At the largest disc currents measured, there is a decrease in the slopes of each plot in Fig. 6, indicating that proportionally less product is being detected at the ring. This is consistent with proportionally less soluble reduced dimer formation, which we attribute to greater film formation and deposition at these higher radical cation concentrations and higher disc potentials. It is interesting that the reduced collection of dimer product persists into the

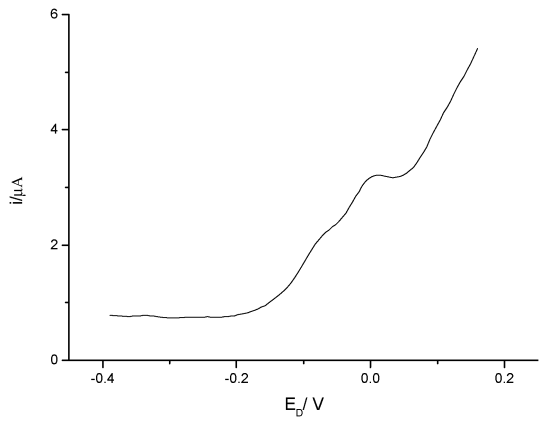

Fig. 4 A typical differential pulse voltammogram at the stationary RDE of the products in a 1 mM solution of indolizine in background electrolyte following prolonged electrooxidation at a disc potential, $E_D > 0.4$ V. The DPV modulation amplitude was 10 mV.

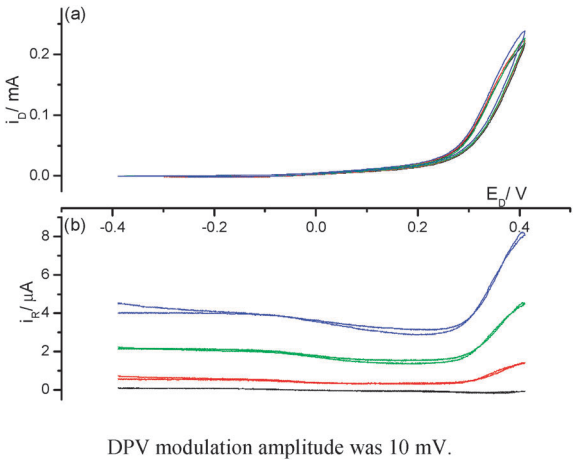

DPV modulation amplitude was 10 mV.

Fig. 5 Typical CVs (v = 20 mV s^{-1}) obtained in the 1 mM indolizine solution from Fig. 4 at the RRDE, rotating at 4 Hz; (a) is the disc current, i_D, response whilst (b) is the ring current, i_R, response observed when cycling the corresponding disc potential, E_D, with the ring potential, E_R, held at −0.140 V (black), −0.040 V (red), +0.060 V (green) and +0.160 V (blue) respectively.

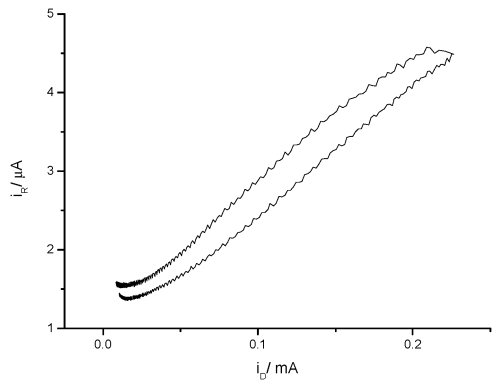

Fig. 6 Plot of i_R *vs.* i_D for E_R = + 0.060 V (the green line in Fig. 5 (b)). Note that the onset of monomer oxidation is near $i_D \approx 0.03$ mA.

reverse sweep of the disc voltammogram and restoration requires disc cleaning; this is consistent with disc film deposition affecting the ring collection efficiency.

The collection efficiencies at the ring of these soluble products have been calculated at each ring potential from the initial linear increase in the ring current with respect to the disc current; these are shown in Fig. 7. Also shown are the calculated E^{θ} and measured (through DPV) $E_{1/2}$ values for the dimers and the soluble products respectively. It is satisfying that the measured collection efficiencies increase in the potential range consistent with the redox potentials of these three dimers, and of the DPV products. This confirms that the soluble products detected in bulk are most likely those formed from the disc electrooxidation reaction, and that they show redox behaviour consistent with that predicted and shown through DPV for the 1,1′- and 1,3′ dimer products. In addition, there is clearly a contribution from a product which oxidises between 0.10 and 0.15 V consistent with the 3,3′- dimer product; we argue that this can be more clearly seen in these experiments than in DPV due to the reduction of the ring current due to monomer oxidation through disc shielding[17a] and the enhanced local concentration of this product at the ring. Semiquantitation (*vide infra*) of these products is also possible at the ring. As both the calculated and measured (for the Fc/Fc^+ reaction) RRDE collection efficiency are N_0 = 0.21, and calculations indicate soluble dimer products undergo a one electron oxidation and to be formed from monomer in a two electron oxidation, the total soluble dimer product detected in Fig. 7 would amount to ~33% of that which could be formed from the monomer radical cation. This is consistent with soluble dimers being a major product of this reaction and that these dimers are the bulk species detected in DPV on prolonged electrooxidation. This proportion of soluble dimer product is also consistent with that expected from the percentage of redox charge previously found in the disc film after CV electrooxidation, especially as this film is thought to be polymeric in nature and result from further electroxidative dimer coupling (*vide infra*), which would reduce the fraction of film redox charge observed. In addition, the amount of the three dimer products detected appears to be comparable; this is consistent with computation, which shows similar monomer radical cation electron spin densities at 1- and 3-positions and predicts energetically that similar proportions of each dimer are likely to be formed.

Indolizine fluorescence

As final evidence to support the presence of soluble dimers in solution, we have exploited the high luminescence of these systems[4d] by characterising the fluorescence emission of the solution after prolonged electrooxidation. Fig. 8 shows the excitation and emission spectra of the resulting soluble products. The excitation spectrum is affected at low wavelength by the inner filter effect of monomer absorption (which has a measured peak excitation of 295 nm in ethanol) however, peak excitation and emission wavelengths of 385 and 445 nm can clearly be seen, consistent with emission from highly fluorescent dimer species at low concentration with characteristically extended electronic conjugation length compared to the monomer.

It is also worth considering the nature of the redox active film product. When oxidising monomer, the disc electrode is at a sufficiently oxidising potential to further oxidise any dimer formed at the electrode surface. The RRDE experiments and calculations are both consistent with the one electron oxidation of dimer products leading to a stable and soluble product; however, given the low redox potential of these species, further oxidation of these dimers is also likely at these potentials. This would give rise to more reactive oxidised dimer species, able to couple and form oligomeric and insoluble species at the electrode surface which themselves could oxidise and couple further on the electrode. Such a mechanism for redox active film formation is found for trimer coupling and indole polymer formation[8] and is also established for pyrroles.[2] Such further oxidation would explain the lack of oxidised dimer detected at the ring (only dimer formed in the gap would escape further oxidation and film formation), the decrease in the proportion of soluble dimer detected at the ring

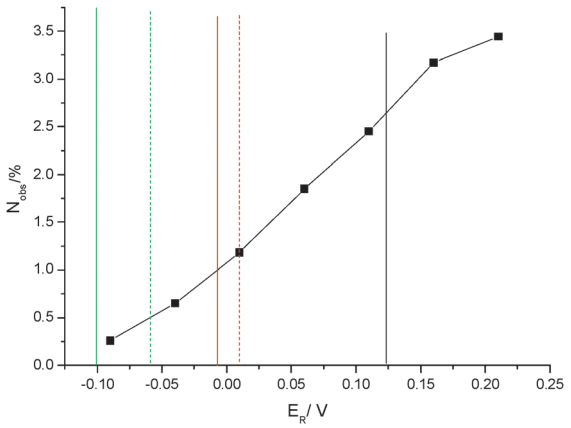

Fig. 7 The calculated collection efficiency, N_{obs}, observed at the ring electrode during voltammetry at the disc electrode of the RRDE as a function of E_R. Solid lines indicate the calculated values of standard dimer reduction potentials, whilst dotted lines indicate the measured values of $E_{1/2}$ obtained for the soluble electrooxidation products obtained from DPV (Fig. 4).

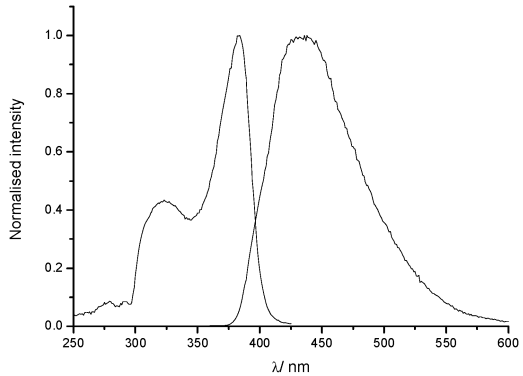

Fig. 8 Normalised fluorescence excitation and emission spectra of the products formed from 1 mM indolizine solution following prolonged electrooxidation. The emission spectrum was measured at a fixed excitation wavelength of 350 nm, whilst the excitation spectrum was measured at a fixed emission wavelength of 435 nm. Note that there is significant perturbation to the excitation spectrum below 320 nm due to adsorption by the relatively high concentration of indolizine monomer present (the inner filter effect).

at higher disc currents (potentials) and the progessive increase in oxidative current seen coincident with monomer oxidation when forming redox films of increasing thickness. It should be noted that some further oxidation could be observed in Fig. 7, particularly at the highest ring potentials, which may complicate definitive quantitation of the amount of each dimer.

Conclusions

This work demonstrates that indolizine is a new class of molecule of interest in the formation of redox active films and novel luminescent products for materials application. It is worth considering the nature of the products of monomer electrooxidation. In general, heteroaromatic monomer oxidation can lead either to redox active oligomer and polymer film formation (such as for pyrroles, thiophenes and furans[2]) or, more unusually, to stable redox active dimer formation, as for indolocarbazole.[4d] The solubility of indolizine is low in acetonitrile and the oxidation potential is also relatively low, which suggests a relatively low radical cation coupling rate. This would favour dimer formation, even in the former case. The electrochemical characteristics show the production of significant amounts of soluble product. Calculations suggest these to be specific dimers, through determining the likely coupling positions of the monomers on oxidation and revealing specific redox behaviour consistent with that observed electrochemically. In the case of indolizine the solubility, redox activity, luminescent conjugation and high degree of delocalisation on oxidation of the dimer products are all consistent with soluble stable redox active dimers being formed. The lack of solubility of the redox active film suggests that this is polymeric and cross linked in nature. We therefore propose that the film is formed through further oxidation and coupling of those dimers formed at or near the electrode surface, as is typically found in the former case. This further oxidation is likely to be favoured at the comparatively high disc electrode potentials required for monomer oxidation. We are currently investigating the synthesis of more soluble functionalised indolizines to assess whether enhanced redox active film formation is observed at higher concentration, as with pyrroles, furans and thiophenes.

This work demonstrates that a combination of computational, spectroscopic and electrochemical measurements can be used to interpret results from the indolizine electrooxidation reaction and indicate the likely coupling products, without the requirement of either complex product or large scale reactant synthesis. As we have shown previously, computation can be used to predict the oxidation potentials and likely coupling positions of heteroaromatics. It is certainly an advantage in this case that each dimer is calculated to have a distinct redox potential, which aids product assignment and quantitation. The use of luminescence spectroscopy, capable of the highly sensitive detection and characterisation of soluble luminescent products has also provided invaluable supporting information. We propose that such an approach can be used as a small scale screening method for the production and characterisation of oligomers formed from other similar luminescent heteroaromatics of interest for electrochemical processes and devices.

Acknowledgements

This work has made use of the resources provided by the EaStCHEM Research Computing Facility (http://www.eastchem.ac.uk/rcf). This facility has been partially supported by the eDIKT initiative (http://www.edikt.org). The School of Chemistry is part of the EaStCHEM joint Chemistry Research School; we acknowledge the financial support of the Scottish Funding Council.

Notes and references

1 (*a*) P. N. Bartlett and J. Farrington, *Bull. Electrochem.*, 1992, **8**, 208; (*b*) S. R. Sivakkumar, N. Angulakshmi and R. J. Sraswathi, *J. Appl. Polym. Sci.*, 2005, **98**, 917; (*c*) A. T. Biegunski, A. Michoti, J. Bukowska and K. Jakowska, *Bioelectrochemistry*, 2006, **69**, 41;

(*d*) J. B. Henry and A. R. Mount, *J. Phys. Chem. A*, 2009, **113**, 13023.
2 (*a*) R. J. Waltman and J. Bargon, *Can. J. Chem.*, 1986, **64**, 76; (*b*) S. Sadki, P. Schottland, N. Brodie and G. Sabouraud, *Chem. Soc. Rev.*, 2000, **29**, 283; (*c*) S. J. Higgins, *Chem. Soc. Rev.*, 1997, **26**, 247.
3 (*a*) S. Yapi Abe, J. C. Bernede, M. A. Delvalle, Y. Tregouet, F. Ragot, F. R. Diaz and S. Lefrant, *Synth. Met.*, 2002, 1261; (*b*) P. Syed Abthagir and R. Saraswathi, *Org. Electron.*, 2004, **5**, 299.
4 (*a*) S. Wakim, J. Bouchard, M. Simard, N. Drolet, Y. Tao and M. Leclerc, *Chem. Mater.*, 2004, **16**, 4386; (*b*) Y. Li, Y. Wu, S. Gardner and B. S. Ong, *Adv. Mater.*, 2005, **17**, 849; (*c*) Y. Wu, Y. Li, S. Gardener and B. S. Ong, *J. Am. Chem. Soc.*, 2005, **127**, 61; (*d*) S. I. Wharton, J. B. Henry, H. McNab and A. R. Mount, *Chem.–Eur. J.*, 2009, **15**, 5482.
5 P. L. T. Boudreault, S. Wakim, N. Blouin, M. Simard, C. Tessier, Y. Tao and M. Leclerc, *J. Am. Chem. Soc.*, 2007, **129**, 9125.
6 (*a*) G. Hua, J. B. Henry, Y. Li, A. R. Mount, A. M. Z. Slawin and J. D. Woollins, *Org. Biomol. Chem.*, 2010, **8**, 1655.
7 D. A. Lerner, P. M. Horowitz and E. M. Evleth, *J. Phys. Chem.*, 1977, **81**, 12.
8 A. R. Mount and A. D. Thomson, *J. Chem. Soc., Faraday Trans.*, 1998, **94**, 553.
9 M. J. Frisch, G. W. Trucks, H. B. Schlegel, G. E. Scuseria, M. A. Robb, J. R. Cheeseman, J. A. Montgomery, Jr., T. Vreven, K. N. Kudin, J. C. Burant, J. M. Millam, S. S. Iyengar, J. Tomasi, V. Barone, B. Mennucci, M. Cossi, G. Scalmani, N. Rega, G. A. Petersson, H. Nakatsuji, M. Hada, M. Ehara, K. Toyota, R. Fukuda, J. Hasegawa, M. Ishida, T. Nakajima, Y. Honda, O. Kitao, H. Nakai, M. Klene, X. Li, J. E. Knox, H. P. Hratchian, J. B. Cross, V. Bakken, C. Adamo, J. Jaramillo, R. Gomperts, R. E. Stratmann, O. Yazyev, A. J. Austin, R. Cammi, C. Pomelli, J. W. Ochterski, P. Y. Ayala, K. Morokuma, G. A. Voth, P. Salvador, J. J. Dannenberg, V. G. Zakrzewski, S. Dapprich, A. D. Daniels, M. C. Strain, O. Farkas, D. K. Malick, A. D. Rabuck, K. Raghavachari, J. B. Foresman, J. V. Ortiz, Q. Cui, A. G. Baboul, S. Clifford, J. Cioslowski, B. B. Stefanov, G. Liu, A. Liashenko, P. Piskorz, I. Komaromi, R. L. Martin, D. J. Fox, T. Keith, M. A. Al-Laham, C. Y. Peng, A. Nanayakkara, M. Challacombe, P. M. W. Gill, B. Johnson, W. Chen, M. W. Wong, C. Gonzalez and J. A. Pople, *Gaussian 03, Revision C.02*, Gaussian, Inc., Wallingford CT, 2004.
10 A. D. Becke, *Phys. Rev. A: At., Mol., Opt. Phys.*, 1988, **38**, 3098.
11 C. Lee, W. Yang and R. G. Parr, *Phys. Rev. B*, 1988, **37**, 785.
12 B. Mennucci and J. Tomasi, *J. Chem. Phys.*, 1997, **106**, 5151.
13 V. Boekelheide and K. J. Fahrenholtz, *J. Am. Chem. Soc.*, 1957, **83**, 458.
14 D. G. Barton, S. L. Soled and E. Iglesia, *Top. Catal.*, 1998, **6**, 87.
15 A. Tschitischibabin, *Chem,. Ber.*, 1927, **60**, 1614.
16 A. J. Bard and L. R. Faulkner, *Electrochemical Methods: Fundamentals and Applications*, John Wiley & Son, New York, 2001.
17 (*a*) A. R. Mount, M. S. Appleton, W. J. Albery, D. Clark and C. E. W. Hahn, *J. Electroanal. Chem.*, 1992, **334**, 155; (*b*) W. J. Albery and S. Bruckenstein, *Trans. Faraday Soc.*, 1966, **62**, 1920.